

A Comparative Analysis of Different Life-Cycle Investment Strategies for Turkey

Ravshanbek Khodzhimatov*, Tolga Umut Kuzubaş, Burak Saltoğlu

Boğaziçi University, Department of Economics, Natuk Birkan Building, 34342 Bebek, Istanbul, Turkey

Abstract

In this paper, we perform a welfare comparison of different life-cycle investment strategies for the pension funds using Monte Carlo simulations in an heterogeneous agent framework for Turkey. We calibrate model parameters based on historical data and compare a set of strategies provided by the pension fund industry and suggested by the asset management literature. Our results reveal that heuristic suggested by Cocco (2004) exhibits a better performance compared to other options. We also show that life-cycle investment strategies outperform “fixed over the lifetime” strategies and risk-averse individuals might hedge their risks by investing in housing.

Keywords: Life-cycle portfolio decisions, human capital, housing, stock market participation

1. Introduction

The field of financial economics has gone through big changes since its foundation by Markowitz [13] and Tobin [19]. Mean-variance analysis suggested that if investors cared about maximizing returns (mean) and minimizing risks (variance), then the optimal share of stocks in a single-period portfolio would be represented by the following equation:

$$\alpha = \frac{\mu - R_f}{\gamma \sigma^2}, \quad (1)$$

where R_f is a risk-free rate, μ and σ^2 are mean and variance of rate of return on stocks, and γ is the parameter of relative risk aversion.

Merton [14] generalized this problem to multiple periods using dynamic programming and found that it is optimal for all households to repeat the same fixed mean-variance solution every period.

However, these results are inconsistent with the popular financial advice suggesting that younger investors should have higher share of stocks in their portfolios, and older investors, higher share of risk-free assets. This advice is summarized by the well-known rule of thumb:

$$\alpha_t = (100 - t)\%, \quad (2)$$

where t is the age of an investor and α_t is the portfolio equity share at age t .

*Corresponding author

Email addresses: rsk@ravshansk.com (Ravshanbek Khodzhimatov), umutkuzubas@gmail.com (Tolga Umut Kuzubaş), burak.saltoglu@gmail.com (Burak Saltoğlu)

Although Samuelson [18] denied that risk-aversion changes by age, dismissing this advice would question the rationality of investors and “constitute *prima facie* evidence that people do not optimize” [6].

Bodie et al. [4] solved this problem by adding human capital into the Merton [14]’s dynamic model and found that for complete markets and risk-free labor income, the optimal share of stocks in a portfolio is given by a generalization of Equation 1:

$$\alpha_t = \frac{\mu - R_f}{\gamma\sigma^2} \left(\frac{F_t + L_t}{F_t} \right), \quad (3)$$

where F_t and L_t are financial and human capital of an agent at age t . Depletion of human capital over the life-cycle relative to the financial wealth produces an optimal investment strategy in the form of a glide path i.e. younger agents carry a higher share of stocks in their portfolio which gradually declines with age. Cocco et al. [9] extended this model for the case of stochastic labor income and obtain a recursive solution where share of stocks for a portfolio constructed age t could be approximated by the following rule of thumb:

$$\alpha_t = \begin{cases} 100\% & t < 40 \\ (200 - 2.5t)\% & t \in [40, 60] \\ 50\% & t > 60 \end{cases} \quad (4)$$

Chang et al. [7] observed that the stock share of a portfolio over the life-cycle exhibits a hump-shaped profile rather than a glide path, which hints the presence of an opposing force. This opposing force is identified as housing investment by Cocco [8], which, due to its large size, crowds out the stock investment from the portfolios of younger agents. Flavin and Yamashita [10] complements this view by providing evidence that younger agents, who already own the house, tend to invest more aggressively, as proposed by Bodie et al. [4].

Munk [15] confirms the same pattern using a series of one-period mean-variance optimizations without relying on dynamic stochastic modeling tools. Finally, Ascheberg et al. [2] illustrated the existence of long-term cointegration among house prices, stock prices, and labor income, a fact predominantly omitted by the literature for the sake of simplicity, which we take into account in our simulations.

In this paper, we compare alternative life-cycle strategies, implemented in the pension fund industry and suggested by the literature using Monte Carlo simulation relying on parameters calibrated for the Turkish economy. Furthermore, we allow for heterogeneity among agents on the dimensions such as sector of work, level of education and risk aversion which enables a thorough welfare comparison of agents with different demographic characteristics.

The remainder of the paper is organized as follows: Section 2 presents the theoretical framework we will use in our simulations. Section 3 provides detailed information on the data sources and calibration. Section 4 compares the simulation results of alternative life-cycle investment strategies and Section 5 concludes.

2. Theoretical framework

2.1. House prices, stock prices and labor income series

Following Campbell et al. [5], we model labor income process as a function of age $f(t)$ plus idiosyncratic shocks v_{it} .¹ Upon reaching the retirement age R , an individual receives a certain percentage λ of his/her last wage. The stochastic labor income process is given as:

$$\log(Y_{i,t}) = \begin{cases} \beta_0 + \beta_1 t + \beta_2 t^2 + \epsilon_{it}, & t < R \\ \beta_0 + \beta_1 R + \beta_2 R^2 + \epsilon_{iR} + \log(\lambda), & t \geq R \end{cases} \quad (5)$$

Furthermore, we assume that labor income, house prices, and stock prices follows geometric brownian motions with drifts μ_L, μ_H, μ_S and volatilities $\sigma_L, \sigma_H, \sigma_S$, satisfying the discrete version of Ascheberg et al. [2]'s correlation structure with nonzero correlations $\rho_{SH}, \rho_{HL}, \rho_{SL}$.²

2.2. Optimal portfolio

Along with the investment strategies, described in Equations 1 - 4, as a benchmark, we consider in the optimal strategy proposed by Munk [15], who showed that the optimal portfolio allocation can be solved analytically³ yielding the following equation for the optimal portfolio shares of assets:

$$\boldsymbol{\pi}' = \frac{1}{\gamma} [(1+l) \cdot (\boldsymbol{\mu}' + \lambda \cdot \mathbf{1}') - \gamma \cdot l \cdot \mathbf{cov}'(\mathbf{r}, r_L)] \boldsymbol{\Sigma}^{-1}, \quad (6)$$

where λ is given by:

$$\lambda = \frac{\gamma + [\gamma \cdot l \cdot \mathbf{cov}'(\mathbf{r}, r_L) - (1+l) \cdot \boldsymbol{\mu}']}{(1+l) \cdot (\mathbf{1}' \boldsymbol{\Sigma}^{-1} \mathbf{1})} \quad (7)$$

2.3. Retirement income

The cash flow in retirement is modeled as the funds invested in the pension plan to be paid back in annuities, not withdrawn immediately. Thus, at the age of retirement $R = 65$, the total wealth W_{65} is used to buy an annuity which will annually repay an individual:

$$A_t = W_{65} \cdot \left(1 + \sum_{t=66}^{100} \frac{p_{t|65}}{(1+r_f)^{t-65}} \right)^{-1} \quad (8)$$

where A_t is the annuity payment at age t , $p_{t|65}$ is the probability of survival at age t , conditional on being alive at the age of 65.

¹We abstract from aggregate shocks, as they solely add an additional source of volatility without affecting our comparative analysis.

²See Appendix B for details.

³Derivation and details of the model are delegated to the Appendix A.

2.4. Welfare measurement

We use stochastic constant relative risk-aversion utility function to compare welfare resulting from different income patterns:

$$E_{65}[U(c_t)] = \sum_{t=66}^{100} \delta^{t-65} \cdot \frac{c_t^{1-\gamma}}{1-\gamma} \cdot p_{t|65} \quad (9)$$

Unlike Cocco et al. [9], we neglect the bequest motives, assuming that a retired agent consumes all of her income at any given time, i.e. $c_t = A_t$.

3. Data and simulation

3.1. Estimation of the Parameters

In this section, we describe the data set used in the parameter calibrations and implement Monte Carlo simulations of the life-cycle portfolios.

We employ monthly data for the Turkish stock market, BIST100,⁴ covering the period 2000–2020, and Turkish housing market, REIDIN⁵, covering the period 2003–2020, to construct stock and house price series. We present time series data for the sample period in Figures 1 and 2.

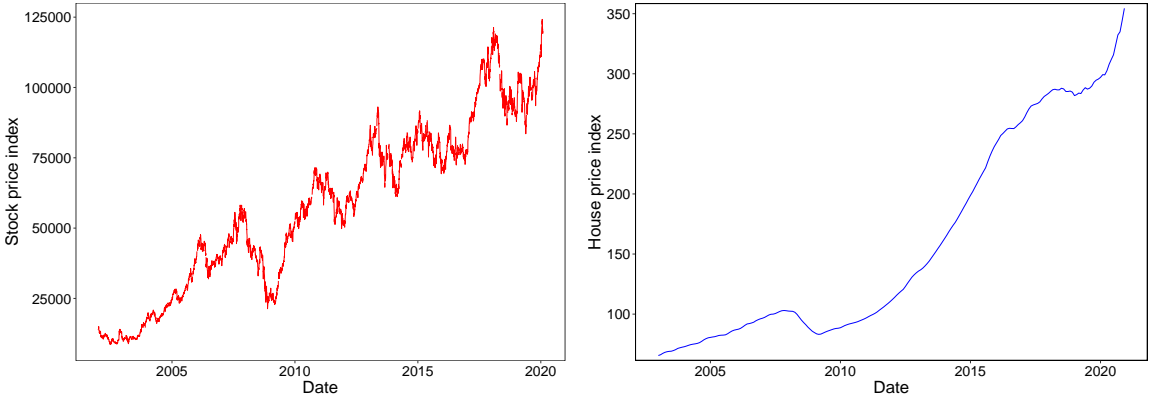


Figure 1: BIST100 Turkish stock market prices

Figure 2: REIDIN Turkish house price index

We construct labor income series using Household Labor Force Survey provided by the Turkish Statistical Institute's [11] which is in the form of a repeated cross-section. In line with Aktuğ et al. [1], we construct a pseudo-panel with 55 thousand data points for 170 households-cohorts for 2002 to 2020. We deflate nominal wages with the consumer price index to obtain real wages. Figure 3 presents life-cycle income profile, which exhibits a hump-shaped pattern consistent with the literature.⁶

In accordance with Munk [15], we run our simulations for a 25-year-old agent who invests in her retirement for 40 years until she reaches retirement at the age of 65. In line with Torul and

⁴BIST100 is an index measuring the stock performance of 100 largest companies in Turkey.

⁵We used residential sales price index for Istanbul calculated using Laspeyres' formula.

⁶See for example Ben-Porath [3].

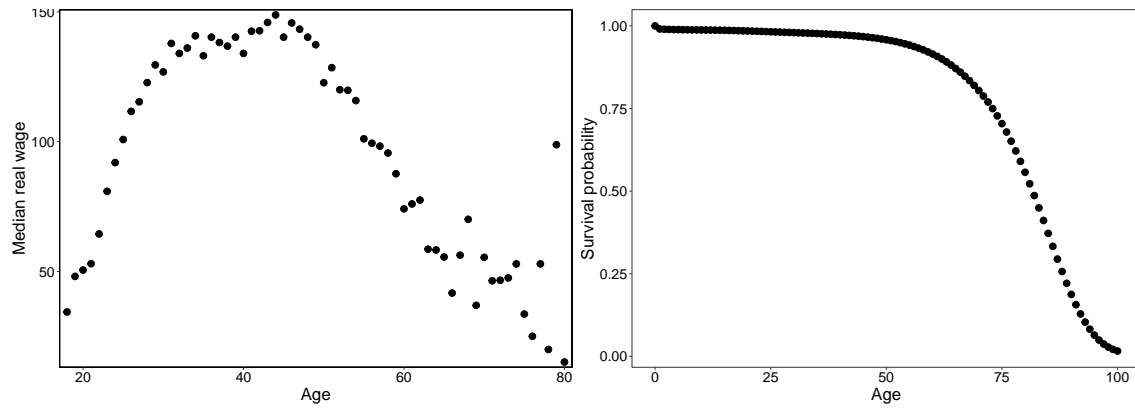


Figure 3: Median Turkish salaries by age

Figure 4: Survival probabilities by age

Oztunali [20], we set the default relative risk aversion coefficient for Turkish households to $\gamma = 1.5$, and the subjective discount rate to $\delta = 0.89$. Survival probabilities for all ages are provided by Turkish Statistical Institute [12] and illustrated in Figure 4.

The drift and volatility parameters for the geometric Brownian motion process governing the rate of return for stocks are estimated as $\mu_S = 11.72\%$ and $\sigma_S = 36.16\%$ respectively. Similarly, for the return process for house prices, drift and volatility are obtained as $\mu_H = 9.84\%$ and $\sigma_H = 3.07\%$. Risk-free rate is set to 12% according to the OECD [16] forecast, and, upon subtracting the medium-term inflation rate forecast 9% provided by the Turkish Central Bank, which gives an annual real interest rate equal to $r_f = 3\%$. The house-stock price and house-wage prices contemporaneous correlations are estimated as $\rho_{SH} = 0.145$ and $\rho_{HL} = 0.117$.

In our simulations, we aim to capture the heterogeneities in the life-cycle wage profiles of agents with different education levels, i.e. stock-wage correlations and different levels of risk aversion by combining the approaches of Olear et al. [17] and Munk [15]. We model the heterogeneity in education based on the differences in wage growth rates. Figure 5 shows the lifetime labor income series for different levels of education. Notice that the curves are hump-shaped over lifetime and are steeper for higher levels of education. We use undergraduate, high school, and primary education, to model “steep”, “moderate”, and “flat” wage dynamics respectively. Performing regressions of wages on age and age squared as given in Equation (10), we estimate growth rates for different education levels⁷

$$\log(wage_t) = \alpha_0 + \alpha_1 \cdot t + \alpha_2 \cdot t^2 + \epsilon_t \quad (10)$$

We model the heterogeneity regarding the sector of work by altering correlations ρ_{SL} between wages and the stock market. Figure 6 illustrates this heterogeneity by plotting median real wages for different sectors along with stock market index to show the differences in the stock-wage correlations. We use three measures of ρ_{SL} in our benchmark: 0, 0.2 and 0.4.

Finally, heterogeneity in terms of different levels of risk aversion is modelled as taking We take $\gamma = 1.5$ as default and perform sensitivity analysis for values $\gamma \in \{1.5, 3, 5, 10\}$ We summarize the

⁷See Appendix C for details of the regression results.

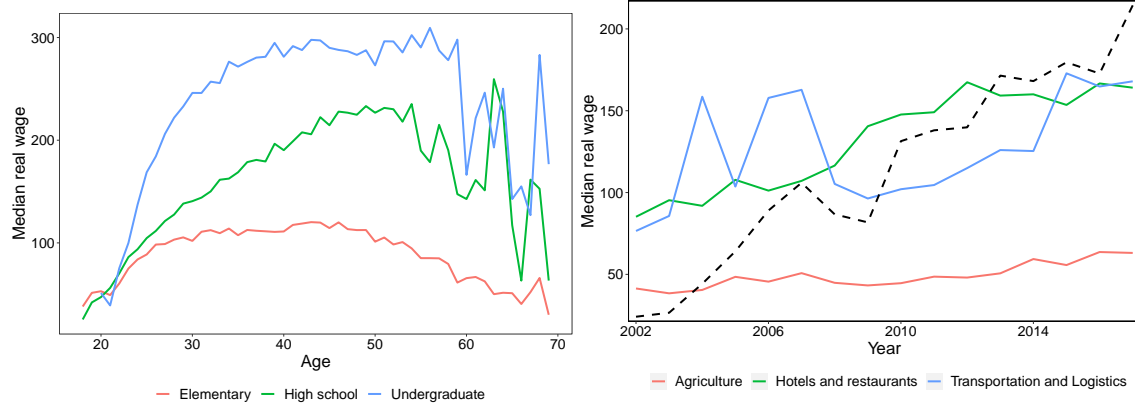


Figure 5: Lifetime real wage dynamics by education level. Figure 6: Historical real wage dynamics by sector. Dashed line shows the normalized stock price index.

Table 1: Benchmark Parameters

Parameter	Description	Value
Y	Beginning age	25
R	Retirement age	65
T	Lifespan (years)	100
γ	Risk aversion	[1.5, 5, 10, 20]
β	Discount rate	0.89
r_f	Risk-free rate	0.03
c	Share of wage invested	0.03
μ_S	Expected stock returns	0.1172
μ_H	Expected housing returns	0.0984
σ_S	Stock returns volatility	0.3616
σ_H	Housing returns volatility	0.0307
ρ_{SH}	House-stock correlation	0.145
ρ_{HL}	House-wage correlation	0.1172
ρ_{SL}	House-wage correlation	[0, 0.2, 0.4]
p_{25}	Survival probability at age 25	0.982
p_{65}	Survival probability at age 65	0.871
p_{100}	Survival probability at age 100	0

benchmark set of parameter values used in the simulations in Table 1.

3.2. Monte Carlo Simulations of Life-cycle Portfolios

Human capital series is constructed as the discounted sum of all future wages until retirement with the discount factor r_f for steep, moderate and flat wage profiles estimated in the previous section. Figure 7 illustrates the evolution of the human capital for flat, moderate, and steep wages for different levels of age.

In order to construct the evolution of the financial capital, we assume that agents invest a certain fraction of her wage in the retirement portfolio which is estimated as 3% for Turkey, by dividing

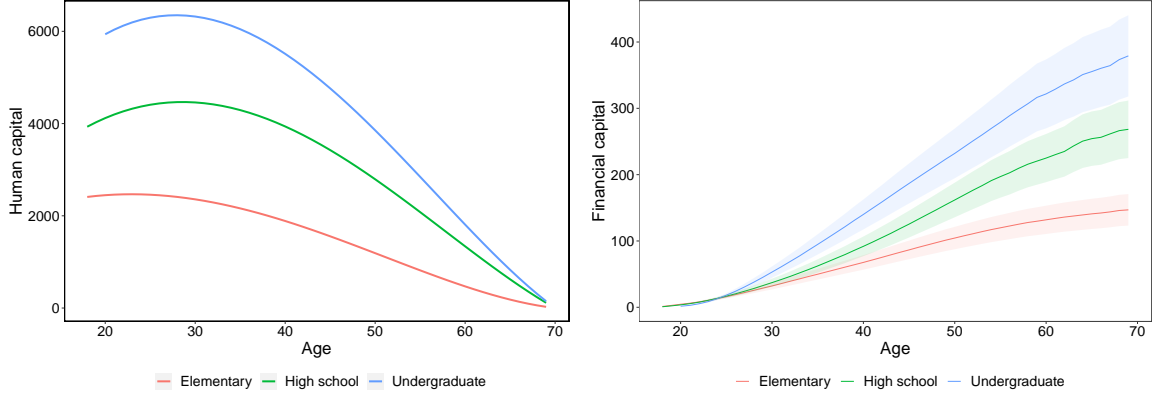


Figure 7: Human capital at every age for individuals with steep, moderate and flat wage growth curves. As individuals get older, their human capital gradually depletes.

Figure 8: Financial wealth accumulation through life, by a naive agent who invests 50% in bonds and 50% in stocks (with 95% confidence intervals).

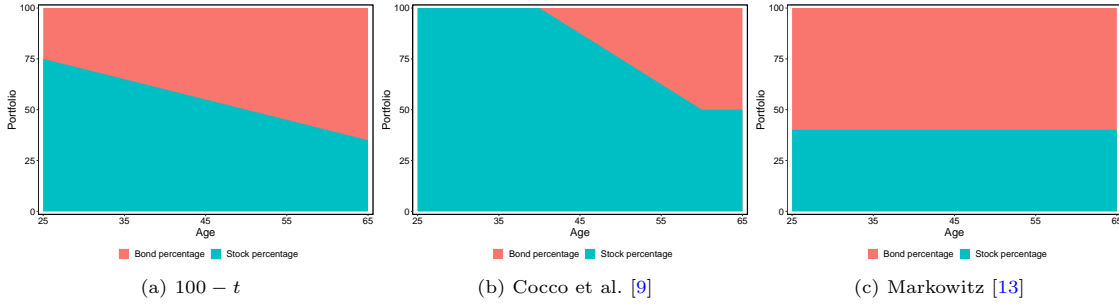


Figure 9: Portfolio allocations at every age, proposed by homogeneous life-cycle strategies

the average contribution to the average wage rate. Previously invested amount accrues a rate of return r_p and the accumulation of the financial capital is given as:

$$F(t) = \sum_{\tau=0}^t c \cdot w_\tau \cdot (1 + r_p)^{t-\tau} \quad (11)$$

In Figure 8 we demonstrate an example of the evolution of financial capital along with the confidence interval for a naive fixed investment strategy, i.e. 50% in stocks and 50% in bonds.

For our simulations, we first describe the investment strategies which propose alternative investment paths for stocks and bonds. The first three options are industry practice such as 100 – age, Cocco (2004) and Markowitz. We illustrate the stock-bond shares for life-cycle allocations calculated based on equations 1, 2 and 4 in Figure 9.

Additionally, we construct the portfolio allocations for the strategies proposed by Bodie et al. [4] (Equation 3) and Munk [15] (Equation 6). These strategies propose younger investors to allocate all of their funds in stocks (or housing), and gradually decrease their share in the portfolio. Figure

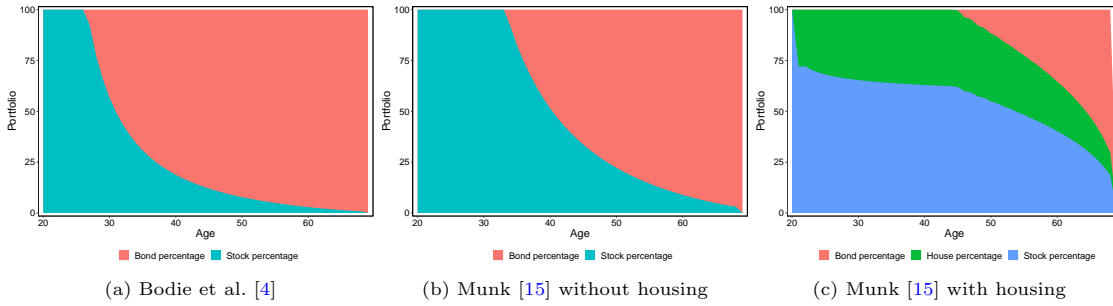


Figure 10: Portfolio allocations suggested by Bodie et al. [4] and [15] (with and without housing). The optimal allocations at every age depend on the previous realizations of volatile stock returns, individual risk-aversion, and wage curves. See Appendix D for details.

10 presents sample portfolio allocations for different strategies.⁸

4. Results

In this section, we provide a comparative analysis of different life-cycle strategies in terms of welfare measured by the expected lifetime utility. Figure 11 presents the box plots of accumulated capital W_{65} at the retirement for six different investment strategies for 10,000 realizations of a Monte Carlo simulation. Figure 12 shows how the results change for different sectors of work and levels of risk-aversion.

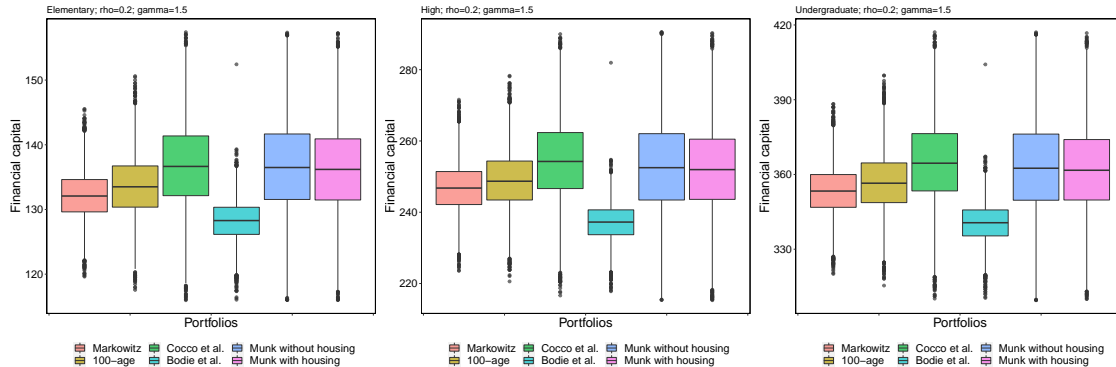


Figure 11: Accumulated capital W_{65} for 6 investment strategies for flat, moderate, and steep income curves.

Retired individuals are assumed to capitalize all of their accumulated wealth to buy annuities and consume them fully i.e. no savings and no bequest motives after the retirement. Annuities and utilities are calculated using Equations 8 and 9 respectively. Figure 13 shows box plots of expected utilities from different scenarios of the Monte Carlo simulation.

Our results reveal that the strategy proposed by Cocco [8] performs better, on average, than any other strategy and even a naive life-cycle investment portfolio $(100 - age)\%$ improves upon the

⁸See Appendix D for a details

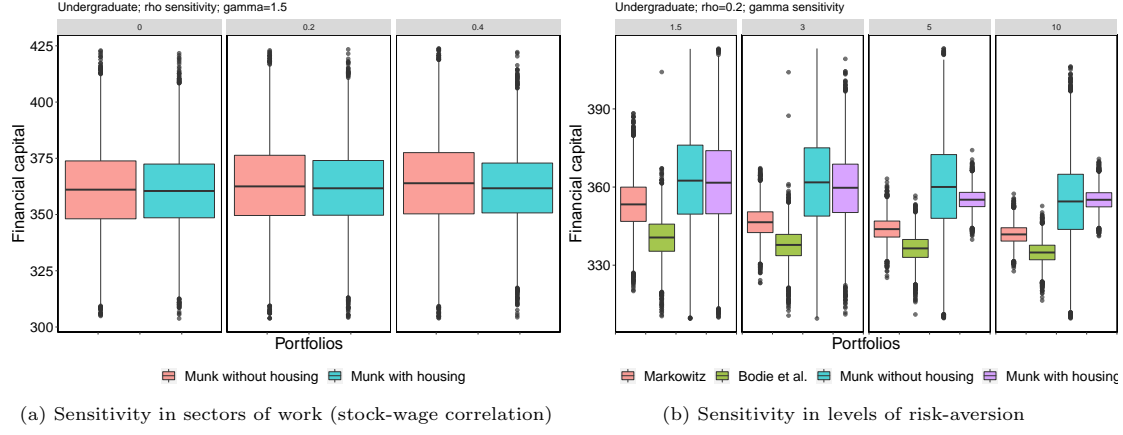


Figure 12: Accumulated capital for different levels of stock-wage correlation and risk-aversion.

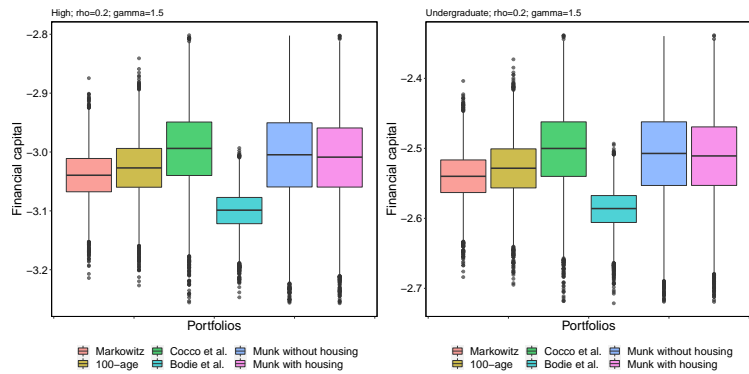


Figure 13: Expected utilities $E_{65}[U(A_t)]$ for 6 investment strategies for flat, moderate, and steep income curves.

fixed-over-lifetime solution by Markowitz [13]. The investment strategy suggested by Bodie et al. [4] exhibit an inferior performance compared to other strategies.

The levels of education, even though results in different levels of welfare, does not change the ranking of alternative investment strategies. A similar pattern is observed for agents working in different sectors.

The strategy proposed by Munk [15], which is based on an optimal portfolio model with an analytical solution, provides a level of welfare at retirement close to Cocco [8] and the strategy with housing, on average, outperforms the one without housing suggesting that risk-averse agents might hedge their risks by investing in housing.

5. Conclusion

In this paper, we present a comparative analysis of alternative life-cycle investment strategies for Turkey using Monte Carlo simulations. Parameters used in the simulations are calibrated/estimated to reflect the properties of the Turkish economy and financial markets. In our simulations, we account for differences in the level of education, sector of work and risk aversion levels. We simulate the lifetime expected utility for the selected strategies which are either proposed by the pension fund industry in the form of heuristics or provided as optimal solutions obtained in a dynamic optimization framework. Our results reveal that, the strategy proposed by Cocco [8] improves upon the alternative strategies. Furthermore, we show that risk averse agents might hedge their risks by investing in housing based on the strategy provided by Munk [15].

References

- [1] Emrehan Aktuğ, Tolga Umut Kuzubaş, and Orhan Torul. Heterogeneity in labor income profiles: evidence from turkey. *Empirical Economics*, 2020.
- [2] M. Ascheberg, H. Kraft, C. Munk, and F. Weiss. The joint dynamics of labor income, stock prices, and house prices and the implications for household decisions. Working papers, Dauphine Universite Paris, International Workshop on Pension, Insurance and Saving, 2013.
- [3] Y. Ben-Porath. The production of human capital and the life-cycle of earnings. *Journal of Political Economy*, 75:352–365, 1967.
- [4] Z. Bodie, R. C. Merton, and W. F. Samuelson. Labor supply flexibility and portfolio choice in a life-cycle model. *Journal of Economic Dynamics and Control*, 16(3):427–449, 1992.
- [5] J. Campbell, J. F. Cocco, F. J. Gomes, and P. J. Maenhout. Investing retirement wealth: A life-cycle model. Working papers, National Bureau of Economic Research, 1999.
- [6] N. Canner, N. G. Mankiw, and D. N. Weil. An asset allocation puzzle. *The American Economic Review*, 87(1):181–191, 1997.
- [7] Y. Chang, J. H. Hong, and M. Karabarbounis. Labor-market uncertainty and portfolio choice puzzles. Working Papers 13, Federal Reserve Bank of Richmond, 2014.
- [8] J. F. Cocco. Portfolio choice in the presence of housing. *The Review of Financial Studies*, 18(2):537–567, 2004.

- [9] J. F. Cocco, F. J. Gomes, and P. J. Maenhout. Consumption and portfolio choice over the life cycle. *The Review of Financial Studies*, 18(2):491–533, 2005.
- [10] M. Flavin and T. Yamashita. Owner-occupied housing and the composition of the household portfolio. *The American Economic Review*, pages 345–362, 2002.
- [11] Turkish Statistical Institute. Household labour force survey, 2012–2017.
- [12] Turkish Statistical Institute. Population and demography, 2020.
- [13] H. Markowitz. Portfolio selection. *The Journal of Finance*, 7(1):77–91, 1952.
- [14] R. C. Merton. Optimum consumption and portfolio rules in a continuous-time model. *Journal of Economic Theory*, 3:373–413, 1971.
- [15] Claus Munk. A mean-variance benchmark for household portfolios over the life cycle. *Journal of Banking and Finance*, 116:105833, 2020. ISSN 0378-4266.
- [16] OECD. Long-term interest rates forecast (indicator), 2018. URL <https://data.oecd.org>.
- [17] G. M. Olear, Frank de Jong, and Ingmar Minderhoud. Individualized life-cycle investing. Design Paper 83, NetSPAR, 2016.
- [18] Paul A. Samuelson. Lifetime portfolio selection by dynamic stochastic programming. *Review of Economics and Statistics*, 51(3):239–246, 1969.
- [19] J. Tobin. Liquidity preference as behavior towards risk. *The Review of Economic Studies*, 25(2):65–86, 1958.
- [20] Orhan Torul and Oguz Oztunali. On income and wealth inequality in Turkey. *Central Bank Review*, 18(3):95–106, 2018.

Appendix A. Derivation of Munk's Constrained Mean-Variance Solution

The dynamic mean-variance problem is created by replacing static wealth W_t with dynamic ratio $\left(\frac{W_{t+1}}{W_t}\right)$. The problem is:

$$\max \left\{ E \left[\frac{W_{t+1}}{W_t} \right] - \frac{\gamma}{2} \text{var} \left(\frac{W_{t+1}}{W_t} \right) \right\} \quad (\text{A.1})$$

We also add the human capital to the model:

$$W_t = F_t + L_t \quad (\text{A.2})$$

Thus, the law of motion is:

$$W_{t+1} = F_t (1 + \boldsymbol{\pi}' \mathbf{r}) + L_t (1 + r_L) \quad (\text{A.3})$$

where $\boldsymbol{\pi}$ is a vector of shares of assets in a portfolio, \mathbf{r} are rates of return on assets, and r_L is the rate of return on human capital, such that $\mathbf{r} \sim (\boldsymbol{\mu}, \boldsymbol{\Sigma})$ and $r_L \sim (\mu_L, \sigma_L)$.

Thus, the moments become:

$$E \left[\frac{W_{t+1}}{W_t} \right] = \frac{1}{1+l} (1 + \boldsymbol{\pi}' \boldsymbol{\mu}) + \frac{l}{1+l} (1 + \mu_L) \quad (\text{A.4})$$

$$\text{var} \left(\frac{W_{t+1}}{W_t} \right) = \left(\frac{1}{1+l} \right)^2 \boldsymbol{\pi}' \boldsymbol{\Sigma} \boldsymbol{\pi} + \left(\frac{l}{1+l} \right)^2 \sigma_L^2 + 2 \frac{l}{(1+l)^2} \cdot \boldsymbol{\pi}' \text{cov}(\mathbf{r}, r_L) \quad (\text{A.5})$$

where $l = \frac{L_t}{F_t}$. Thus, we can rewrite Equation A.1 as:

$$\max_{\boldsymbol{\pi}} \left\{ \frac{1}{1+l} ((1 + \boldsymbol{\pi}' \boldsymbol{\mu}) + l (1 + \mu_L)) - \frac{\gamma}{2(1+l)^2} \cdot (\boldsymbol{\pi}' \boldsymbol{\Sigma} \boldsymbol{\pi} + l^2 \sigma_L^2 + 2l \cdot \boldsymbol{\pi}' \text{cov}(\mathbf{r}, r_L)) \right\} \quad (\text{A.6})$$

Cancelling out redundant elements, our optimization problem takes the following form:

$$\max_{\boldsymbol{\pi}} \left\{ \boldsymbol{\pi}' \boldsymbol{\mu} - \frac{\gamma}{2(1+l)} \cdot (\boldsymbol{\pi}' \boldsymbol{\Sigma} \boldsymbol{\pi} + 2l \cdot \boldsymbol{\pi}' \text{cov}(\mathbf{r}, r_L)) \right\} \quad (\text{A.7})$$

subject to:

$$\boldsymbol{\pi}' \mathbf{1} = 1 \quad (\text{A.8})$$

$$-\pi_i \leq 0, \forall i \quad (\text{A.9})$$

The Lagrangean is:

$$L = \boldsymbol{\pi}' \boldsymbol{\mu} - \frac{\gamma}{2(1+l)} \cdot (\boldsymbol{\pi}' \boldsymbol{\Sigma} \boldsymbol{\pi} + 2l \cdot \boldsymbol{\pi}' \text{cov}(\mathbf{r}, r_L)) + \lambda \cdot (\boldsymbol{\pi}' \mathbf{1} - 1) - \boldsymbol{\psi}' \boldsymbol{\pi}, \quad (\text{A.10})$$

where $\boldsymbol{\psi}$ is a vector of Lagrange coefficients for non-negativity constraints for all π_i . Karush-Kuhn-Tucker conditions are:

$$\frac{\partial L}{\partial \boldsymbol{\pi}_{(\psi_i \geq 0)}} \geq 0 \quad (\text{A.11})$$

$$\pi_i \cdot \frac{\partial L}{\partial \pi_i_{(\psi_i = 0)}} = 0 \quad (\text{A.12})$$

$$\boldsymbol{\pi}' \mathbf{1} = 1 \quad (\text{A.13})$$

$$\psi_i \cdot \pi_i = 0 \quad (\text{A.14})$$

$$\pi_i, \psi_i, \lambda \geq 0 \quad (\text{A.15})$$

for all i . Equation A.11 yields:

$$\boldsymbol{\mu}' - \frac{\gamma}{2(1+l)} \cdot (2\boldsymbol{\pi}' \boldsymbol{\Sigma} + 2l \cdot \mathbf{cov}'(\mathbf{r}, r_L)) + \lambda \cdot \mathbf{1}' - \boldsymbol{\psi}' = 0 \quad (\text{A.16})$$

which is equivalent to:

$$\boldsymbol{\pi}' = \frac{1}{\gamma} [(1+l) \cdot (\boldsymbol{\mu}' + \lambda \cdot \mathbf{1}' - \boldsymbol{\psi}') - \gamma \cdot l \cdot \mathbf{cov}'(\mathbf{r}, r_L)] \boldsymbol{\Sigma}^{-1} \quad (\text{A.17})$$

Substituting this into Equation A.13 we obtain:

$$\boldsymbol{\pi}' \mathbf{1} = \frac{1}{\gamma} [(1+l) \cdot (\boldsymbol{\mu}' + \lambda \cdot \mathbf{1}' - \boldsymbol{\psi}') - \gamma \cdot l \cdot \mathbf{cov}'(\mathbf{r}, r_L)] \boldsymbol{\Sigma}^{-1} \mathbf{1} = 1 \quad (\text{A.18})$$

which yields:

$$\lambda = \frac{\gamma + [\gamma \cdot l \cdot \mathbf{cov}'(\mathbf{r}, r_L) + (1+l) \cdot \boldsymbol{\psi}' - (1+l) \cdot \boldsymbol{\mu}']}{(1+l) \cdot (\mathbf{1}' \boldsymbol{\Sigma}^{-1} \mathbf{1})} \quad (\text{A.19})$$

When $\pi_i > 0$ we use the Equations A.17 and A.18 with $\psi_i = 0$. Otherwise, $\psi_i > 0$ and:

$$\frac{\partial L}{\partial \pi_i_{(\psi_i=0)}} > \frac{\partial L}{\partial \pi_i_{(\psi_i>0)}} = 0, \quad (\text{A.20})$$

which, combined with Condition A.12 forces $\pi_i = 0$. Next, we reduce the dimension of the problem and solve for nonnegative values.

Appendix B. Ascheberg's correlation structure

The structure that returns desired correlation coefficients ρ_{SL} , ρ_{SH} and ρ_{HL} is as follows:

$$\frac{\Delta S_{t+1}}{S_t} = \mu_S + \sigma_S \cdot \epsilon_{St} \quad (\text{B.1})$$

$$\frac{\Delta H_{t+1}}{H_t} = \mu_H + \sigma_H \cdot \left(\epsilon_{St} \rho_{SH} + \epsilon_{Ht} \sqrt{1 - \rho_{SL}^2} \right) \quad (\text{B.2})$$

$$\frac{\Delta Y_{t+1}}{Y_t} = \mu_L + \sigma_L \cdot \left(\epsilon_{St} \rho_{SL} + \epsilon_{Ht} \frac{\rho_{HL} - \rho_{SH} \rho_{SL}}{\sqrt{1 - \rho_{SH}^2}} + \epsilon_{Lt} \sqrt{1 - \rho_{SL}^2 - \left(\frac{\rho_{HL} - \rho_{SH} \rho_{SL}}{\sqrt{1 - \rho_{SH}^2}} \right)^2} \right) \quad (\text{B.3})$$

To derive this, let Σ be a correlation matrix of a vector $X = (x_1, x_2, \dots, x_K)$. Also, let $\Sigma = LL'$ be a Cholesky decomposition of this matrix.

Notice that the variance-covariance matrix of an i.i.d. random vector $\Omega = (\epsilon_1, \epsilon_2, \dots, \epsilon_K)$ with variances equal to 1, is an identity matrix. Thus, the product $L\Omega$ has the same correlation structure as X :

$$\text{cov}(L\Omega) = E[(L\Omega)(L\Omega)'] = E[L\Omega\Omega'L'] = L \cdot E[\Omega\Omega'] \cdot L' = L \cdot \text{var}(\Omega) \cdot L' = L \cdot I \cdot L' = LL' = \Sigma \quad (\text{B.4})$$

The conclusion comes from the fact that the Cholesky decomposition of a correlation matrix R :

$$R = \begin{bmatrix} 1 & \rho_{SH} & \rho_{SL} \\ \rho_{SH} & 1 & \rho_{HL} \\ \rho_{SL} & \rho_{HL} & 1 \end{bmatrix}$$

can be easily calculated to be equal to Q :

$$Q = \begin{bmatrix} 1 & 0 & 0 \\ \rho_{SH} & \sqrt{1 - \rho_{SH}^2} & 0 \\ \rho_{SL} & \frac{\rho_{HL} - \rho_{SH} \rho_{SL}}{\sqrt{1 - \rho_{SH}^2}} & \sqrt{1 - \rho_{SL}^2 - \left(\frac{\rho_{HL} - \rho_{SH} \rho_{SL}}{\sqrt{1 - \rho_{SH}^2}} \right)^2} \end{bmatrix}$$

Appendix C. Wage regression

The regressions of log wages by age return the following coefficients.

Table C.2: Wage regression results by age

	flat	moderate	steep
(intercept)	-91.095092	-294.4476	-395.0145
age	9.950874	21.4301	29.9319
age ²	-0.119622	-0.2249	-0.3196

The log wages can be calculated using these coefficients. Figure C.14 illustrates how the estimated rates fit the data:

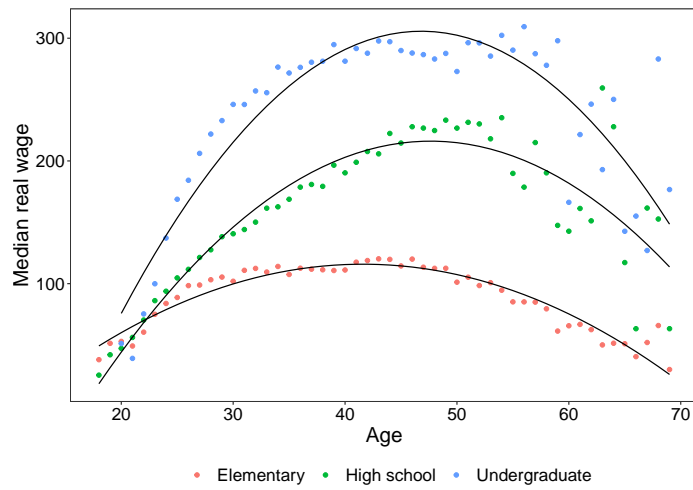


Figure C.14: Fitted values from wage regressions

Appendix D. Portfolio allocations

In this section we present portfolio allocations for individualized life-cycle strategies for heterogeneous individuals, mentioned in the article.

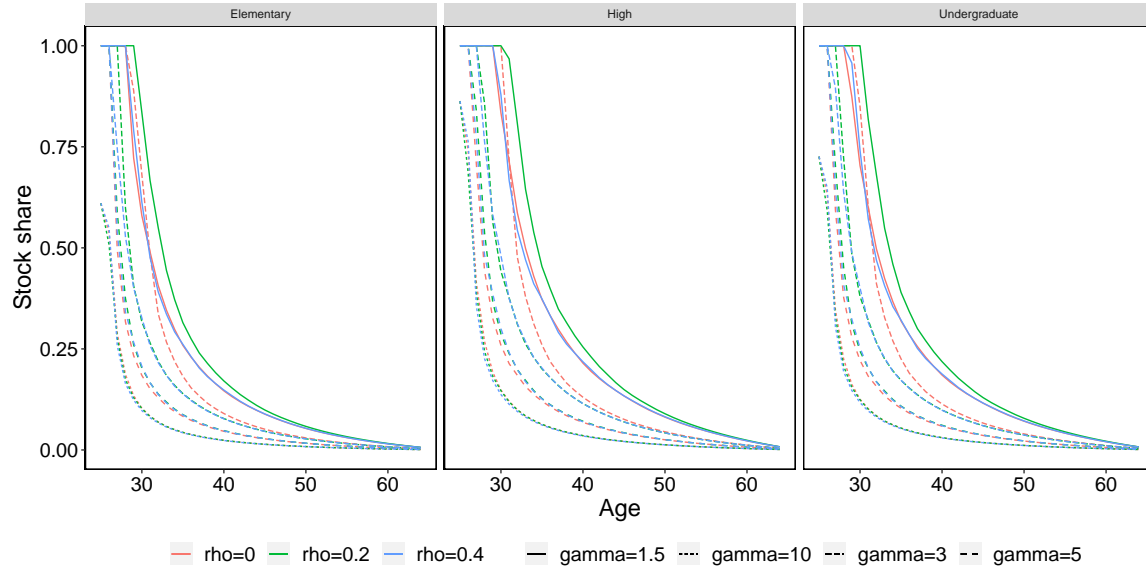


Figure D.15: Stock shares by age for Bodie et al. [4]

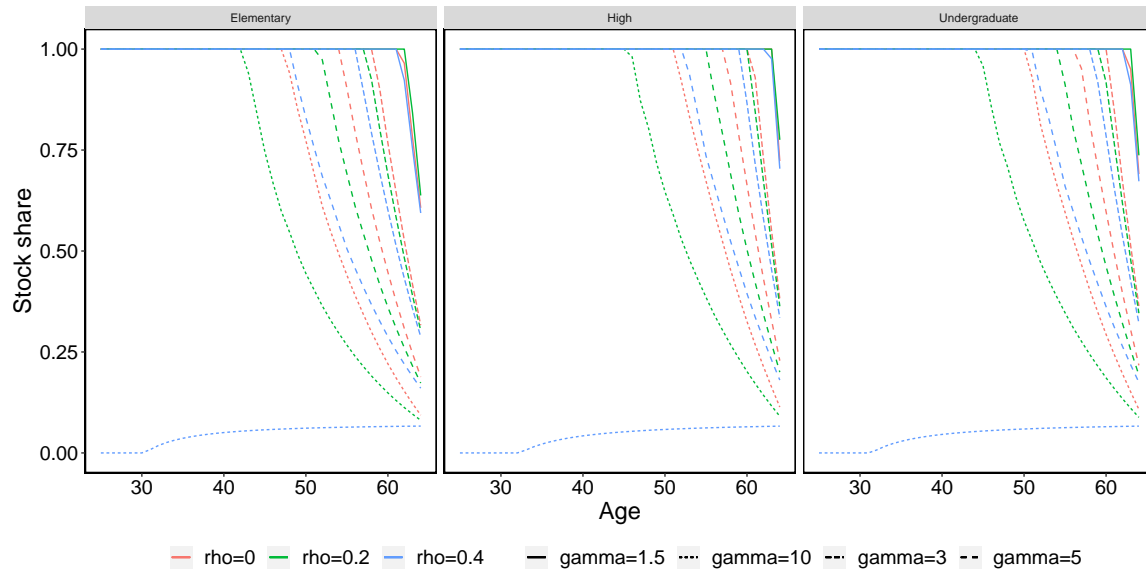


Figure D.16: Stock shares by age for Munk [15] without housing

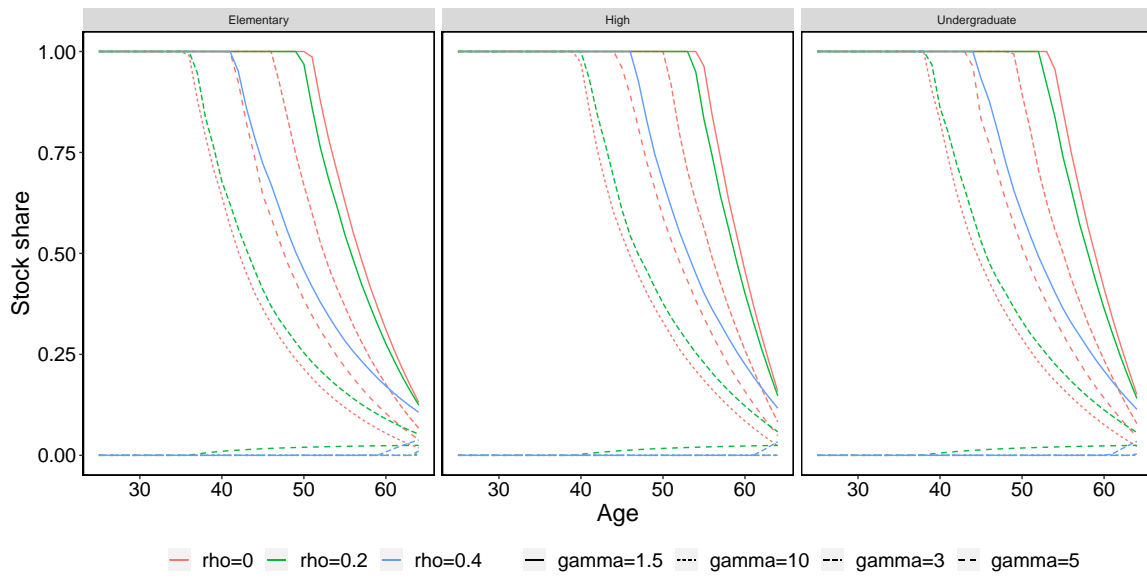


Figure D.17: Stock shares by age for Munk [15] with housing

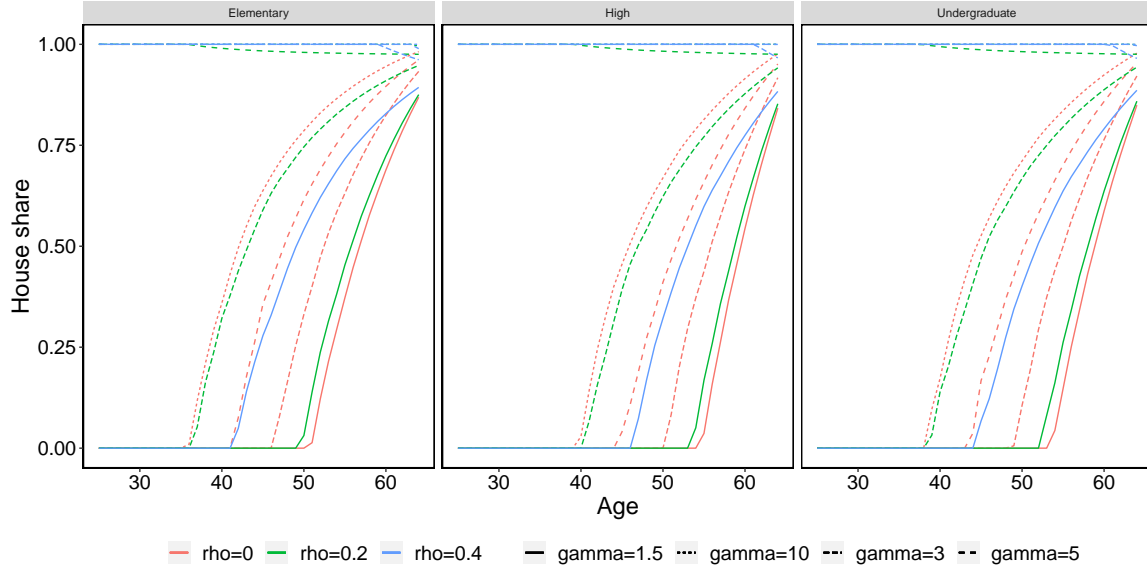


Figure D.18: House shares by age for Munk [15] with housing